A Study of Three-Phase Four Switch Inverter with Synchronous Reference Frame-Based Fuzzy Logic Controller Using for Grid-Connected PV System

Golkonda Anitha, Research Scholar, University College of Engineering, Osmania University, Hyderabad, India, Email: mahanithagolkonda11@gmail.com

K. Krishnaveni, Professor, Chaitanya Bharati Institute of Technology, Hyderabad, India, Email: krishnaveni_eee@cbit.ac.in

G. Yesuratnam, Sr. Professor, University College of Engineering, Osmania University, Hyderabad, India, Email: ratnamgy2003@gmail.com

Abstract - **The advancement in inverter topology has led to the development of the Three-Phase Four-Switch (TPFS) inverter, which minimizes losses, reduces complexity, and lowers costs. This compact and cost-effective solution offers improved performance, making it an attractive option for a wide range of applications. The TPFS inverter must synchronize its output with the grid's voltage and frequency when connected to the grid. This paper introduces a novel Fuzzy Logic Controller (FLC) designed to optimize the performance of a TPFS inverter. The key design considerations of this system include Maximum Power Point Tracking (MPPT) control, grid synchronization, and maintaining a Total Harmonic Distortion (THD) within permissible limits. The proposed approach uses a TPFS inverter instead of a traditional Three-Phase Six-Switch (TPSS) inverter for grid-connected PV systems. The FLC with TSFS inverter is simulated and compared to a conventional Synchronous Reference Frame (SRF) based Proportional Integral (PI) controller. It was found that the proposed FLC is more robust than the SRF-PI controller in terms of cost reduction and low THD. A Space Vector Pulse Width Modulation (SVPWM) control algorithm is proposed for the TPFS inverter inspired by the operating principles of the TPSS inverter. The TPSS inverter divides the $\alpha\beta$ plane into six sectors, and the necessary reference voltage space vector is formed using effective (mean) vectors. This principle forms the basis of the space vector PWM algorithm for the grid-connected TPFS inverter using Clarke's Transformation.**

Keywords —: Three-Phase Four-Switch (TPFS) Inverter, Three-Phase Six-Switch (TPSS) Inverter, Space Vector Pulse Width Modulation (SVPWM), Synchronous Reference Frame (SRF) controller, Fuzzy Logic Controller (FLC)

I. INTRODUCTION

Over the years, Three-Phase Six-Switch (TPSS) inverters have been the traditional choice for variable-speed Alternating Current (AC) motor drives. However, recent research has explored the potential of Three-Phase Four-Switch (TPFS) inverters for uninterruptible power supply and variable speed drives. [1]- [2]. The growing interest in TPFS inverters can be attributed to their numerous advantages over traditional TPSS inverters. One major benefit is the reduced cost due to fewer switches, leading to lower switching and conduction losses. Additionally, TPFS inverters have simplified interface circuits and logic signal supply for switches, making them easier to control. The control algorithms for logic signal generation are also simpler, reducing the computational burden. Furthermore,

the minimized switch interaction in TPFS inverters reduces the risk of switch damage. The three-phase inverter with four switches, proposed by Van der Broeck and Van Wyk [3], aimed to minimize component costs. This configuration is referred to as the Three-Phase Four-Switch (TPFS) or (B4) inverter, distinguishing it from the conventional B6 inverter, as illustrated in Figure 1.

It has one power leg comprising two serial capacitors and two switching legs, each containing two IGBT switches with the phase 'a' connecting to the midpoint of the two DC-link capacitors and the phases 'b' and 'c' connected to the two inverter legs. The primary challenge in TPFS inverters is the voltage balancing of DC-link capacitors, as it directly impacts the output current harmonics. The voltage imbalance issue may arise due to the inherent four-switch structure. To

address this problem, several studies have proposed modifying traditional modulation strategies by introducing additional constraints [4],[5],[6]-[7]. Previous studies have investigated the application of Fuzzy Logic Controller (FLC)-based Induction Motor (IM) drives [8]-[9]. Additionally, a few works have explored the integration of FLC with Space Vector Pulse Width Modulation (SVPWM) for Three-Phase Four-Switch (TPFS) inverters in grid-connected Photovoltaic (PV) systems. The main contribution of this paper is to propose a new SRF-FLC of a three-phase four-switch inverter with a grid-connected PV system compared with other works to investigate the dynamic performance of the TPFS inverter using the FLC.
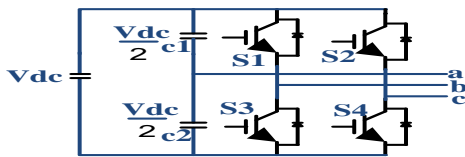

Figure 1 Three-Phase Four-Switch Inverter

This paper makes the following key contributions: 1) investigating the performance of a TPFS inverter using SRF-FLC, 2) validating the proposed SRF-FLC through simulations by comparing it with the conventional SRF-PI controller, and 3) comparing the performance of the proposed TPFS inverter and the TPSS inverter using THD. The discussed topology has a PV Array, MPPT Perturb and Observe (P&O) Algorithm, and Boost Converter. This paper also suggests a modified SVM strategy, adapted to the proposed converter, to eliminate the effect of the voltage imbalance problem of capacitors. MATLAB/Simulation has been done to evaluate this topology's performance and compare simulation results with past works.

II. SPACE VECTOR MODULATION

The method for producing PWM signals that regulate the voltage applied to the motor phases is referred to as SVPWM. It has several benefits compared to conventional PWM methods, including reduced switching losses, greater DC bus voltage consumption and enhanced harmonic performance. From Figure 1 the switching status is denoted by binary variables S1 to S4, which are set to "1" when the switch is closed and "0" when open. In addition, the switches in one inverter branch are controlled complementary (1 on, off), therefore:

$$S1+S2=1$$
$$S3+S4=1 \qquad (1)$$

The output voltages Van, Vbn, and Vcn of the inverter in the form of switching states are given by Equations (2)-(4):

$$Van = \frac{Vdc}{3}[4S1 - 2S2 - 1] \qquad (2)$$

$$Vbn = \frac{Vdc}{3}[4S2 - 2S1 - 1] \qquad (3)$$

$$Vcn = \frac{2Vdc}{3}[1 - S1 - S2] \qquad (4)$$

The combinations of switching states (S1-S4) result in four general space vectors (Table 1). The components of these space vectors are obtained from the abc voltages using Clark's transformation, which converts the three-phase voltages into a two-dimensional representation displayed in Equation (5).

$$\begin{bmatrix} V_d \\ V_q \end{bmatrix} = \frac{2}{3} \begin{bmatrix} 1 & -\frac{1}{2} & -\frac{1}{2} \\ 0 & \frac{\sqrt{3}}{2} & -\frac{\sqrt{3}}{2} \end{bmatrix} \begin{bmatrix} Va \\ Vb \\ Vc \end{bmatrix} \qquad (5)$$

The Vref and angle (α) are given as in the Equations (6) & (7)

$$|Vref| = \sqrt{V_d^2 + V_q^2} \qquad (6)$$

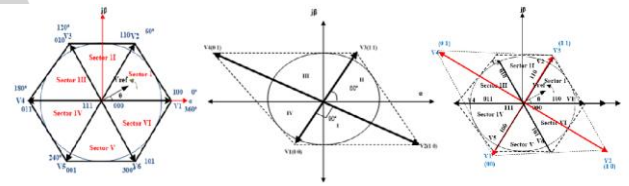$$\alpha = \tan^{-1}(\frac{Vq}{Vd}) \qquad (7)$$

Figure 2 SV diagram of (a) TPSS inverter (b) TPFS inverter (c) comparative analysis of SVPWM

Figures 2 (a) and (b) show the space vector diagram of the TPSS inverter where $\alpha\beta$ plane is divided into six sectors and four sectors for the TPFS inverter, and Figure 2(c) indicates the comparative analysis of both inverters [10].

The SVPWM technique for a four-switch three-phase inverter is derived from the principle of similarity with a six-switch inverter, where the plane is divided into four sectors instead of six, each corresponding to a unique vector [11]-[12]. The active vectors and their durations in a sampling interval are chosen and calculated for these sectors V1, V2, V3, and V4 based on the location of Vref. For a four-switch inverter, the active vectors are divided into four vectors named V1, V2, V3, and V4. The duration of these vectors in a sampling interval is calculated using Vref location [13]-[14]. After calculating vectors V1, V2, V3, and V4 vectors which divide the $\alpha\beta$ Plane into four sectors and each sector is of 90°.

Each sector represents a specific range of voltage vector angles, determining the appropriate switching sequence for the inverter's power switches. Table I indicates the switching states and voltage components for the TPFS Inverter.

Table I   Switching vectors, Phase, and line voltages

Voltage vectors	Switching Vectors		Phase Voltages			Line-voltages		
	a	b	Van	Vbn	Vcn	Vab	Vbc	Vca
V₁	0	0	-1/3	-1/3	2/3	0	-1	1
V₂	1	0	1	-1	0	2	-1	-1
V₃	1	1	1/3	1/3	-2/3	0	1	-1
V₄	0	1	-1	1	0	-2	1	1

Table II   Sectors and Range of Angles

Sector	Range of Angle	Space Vectors
1	-120°<α<-30°	$\frac{2}{3}\angle -120°$
2	-30°<α<60°	$\frac{2}{\sqrt{3}}\angle -30°$
3	60°<α<150°	$\frac{2}{3}\angle 60°$
4	150°<α<-120°	$\frac{2}{\sqrt{3}}\angle 150°$

Calculation of each Sectors angle difference and Range of angles are shown in Table II.

III. STRUCTURE OF THE GRID-CONNECTED PV SYSTEM WITH THE TPFS INVERTER

A TPFS inverter with SRF-FL Controller comprises of a PVA system, MPPT controller, SRF-FL controller, and Grid. PVA is connected to the Boost Converter through the MPPT controller. After maximum power extraction of the PVA, the boost converter is connected to a four-switch inverter. The output of the TPFS inverter is connected to an LC filter for harmonics compensation and further connected to the grid.

A. Photo Voltaic Array (PVA)

A solar photovoltaic (PV) cell, commonly known as a solar cell, is a device that converts sunlight directly into electricity through the photovoltaic effect [15]. The Photo Voltaic Array (PVA) is designed with a specific combination of series and parallel panels to generate the required voltage Vpv and current Ipv for the B4 inverter to inject power into the grid. A boost converter is necessary to achieve maximum power extraction from the PVA and maintain a stable DC voltage.

B. Maximum Power Point Tracking (MPPT)

MPPT is an efficient DC-to-DC converter used to maximize the power output of a solar system. Due to the fluctuating sunlight intensity (irradiance) throughout the day, solar panels experience continuous variations in voltage and current output. To optimize energy harvesting, Maximum Power Point Tracking (MPPT) algorithms systematically sweep through the panel voltage range to identify the optimal combination of voltage and current, known as the 'sweet spot', which yields maximum power output. The MPPT controller continually monitors and adjusts the PV voltage to ensure maximum power generation. The boost converter is controlled by the P&O MPPT method, a fast and simple technique for controlling the converter [16]. After maximum power extraction of the PVA power, the boost converter is connected to a three-phase four-switch inverter. The following flowchart provides a visual representation of the Perturb and Observe (P&O) algorithm is shown in Figure 3.
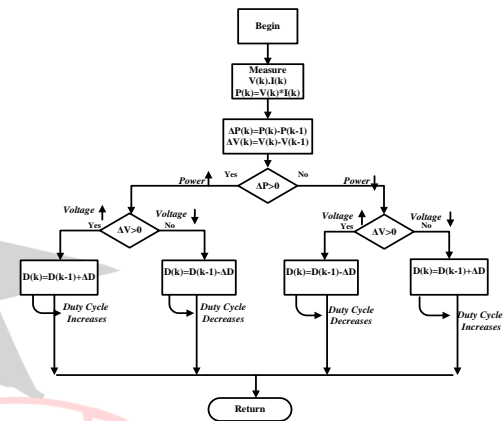

Figure 3 P&O algorithm for MPPT technique

A. Boost converter

The conventional DC-DC boost converter circuit configuration is illustrated in Figure 4, which shows the typical topology of a boost converter, including the power switch (IGBT), diode, inductor, and capacitor. Here input for the boost converter is from a solar PV cell that acts as a DC input voltage source Vin, a controllable IGBT switch, an inductor L, a capacitor C, a load resistor R, and a PWM block.Vo represents the voltage across the capacitor and I_L represents the current through the inductor.

The duty ratio of the boost converter switch is adjusted based on changes in PVA voltage and current determined by the MPPT technique. These values vary according to changes in the solar irradiation.
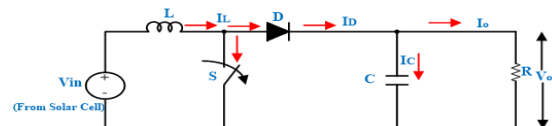

Figure 4 PV connected Boost converter

B. Synchronous Reference Frame

For sharing the PVA power to the grid, synchronization of three-phase voltages needs to be done where the voltage amplitude, frequency, and phase need to be matched. To achieve this Synchronous Reference Frame (SRF) controller

is integrated into the TPFS inverter [17], [18] [19]. The SRF controller operates by taking feedback from grid and inverter voltages and currents respectively. The SRF controller is the finest control module for the integration of renewable sources into the grid. The SRF control structure is very simple and has a less complex mathematical model which helps the controller with faster response [20]. The SRF controller is generally used for generating reference voltages to any PWM technique controlling the voltage source inverter. The SRF controller takes feedback from the grid phase voltages and TPFS inverter currents (in per unit representation) and calculates the reference signals [21]-[22]. The complete structure of the SRF controller can be observed in Figure 5.

The magnitude, frequency, and phase of the TPFS inverter output voltages are controlled by the SRF reference signals making it follow the grid. For generating the Sine reference signals the complete controller is designed in d-q component format using Park's transformation equations given below:
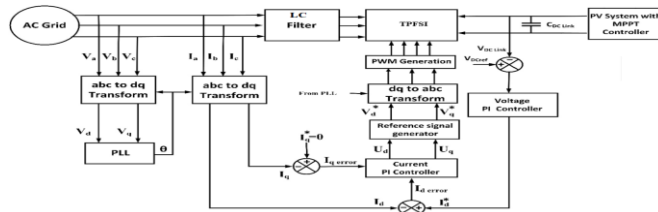
Figure 5 SRF control structure with grid and inverter feedback

$$\begin{bmatrix} F_d \\ F_q \end{bmatrix} = \frac{2}{3}\begin{bmatrix} Sin\,wt & Sin\left(wt - \frac{2\pi}{3}\right) & Sin\left(wt + \frac{2\pi}{3}\right) \\ Cos\,wt & Cos\left(wt - \frac{2\pi}{3}\right) & Cos\left(wt + \frac{2\pi}{3}\right) \end{bmatrix}\begin{bmatrix} F_a \\ F_b \\ F_c \end{bmatrix} \quad (10)$$

In the given expression (10), 'F' represents any signal either voltage 'V' or current 'I'. 'wt' is the phase angle of the grid voltage of phase 'a' determined by Phase Locked Loop (PLL) [23]-[24]. The voltage d-q components for the generation of reference signals are expressed as:

$$\vartheta_d^* = Ud + \vartheta d + L\omega i_q \quad (11)$$

$$\vartheta_q^* = Uq + \vartheta q - L\omega i_d \quad (12)$$

Here, $\vartheta d\,\vartheta q$ and $i_d i_q$ are determined by equation (10) which are the grid voltages and inverter currents d-q components. The Ud and Uq components are determined by the current controller (PI controller) with input taken from error dq current components as expressed below.

$$Ud = \left(i_{d\,ref} - i_d\right)\left(K_{pi} + \frac{K_{ii}}{s}\right) \quad (13)$$

$$Uq = \left(i_{q\,ref} - i_q\right)\left(K_{pi} + \frac{K_{ii}}{s}\right) \quad (14)$$

Here, $i_{d\,ref}\,i_{q\,ref}$ are the reference dq current components. $K_{pi}\,K_{ii}$ are the proportional and integral gains of the current

controller determined by the trial-and-error method. The $i_{q\,ref}$ is zero and the $i_{d\,ref}$ is expressed as:

$$i_{d\,ref} = \left(\vartheta_{dc\,ref} - \vartheta_{dc}\right)\left(K_{pv} + \frac{K_{iv}}{s}\right) \quad (15)$$

Here, $\vartheta_{dc\,ref}$ is the reference DC link voltage input to the four-switch inverter. $K_{pv}\,K_{iv}$ are the proportional and integral gains of the voltage controller tuned as per the response of the controller. The reference signals generated by the expressions (11) and (12) are converted to Sine signals using inverse Park's expressions given as:

$$\begin{bmatrix} \vartheta_a \\ \vartheta_b \\ \vartheta_c \end{bmatrix} = \begin{bmatrix} Sin\,wt & Cos\,wt \\ Sin\left(wt - \frac{2\pi}{3}\right) & Cos\left(wt - \frac{2\pi}{3}\right) \\ Sin\left(wt + \frac{2\pi}{3}\right) & Cos\left(wt + \frac{2\pi}{3}\right) \end{bmatrix}\begin{bmatrix} \vartheta_d \\ \vartheta_q \end{bmatrix} \quad (16)$$

The final reference signals $\vartheta_a\,\vartheta_b\,\vartheta_c$ are given input to the TPFS Inverter to determine the V$_{ref}$ signal for the generation of pulses to the four switches.

C. Fuzzy Logic Controller (FLC)

FLC block generates the voltage reference value for the SVPWM technique to generate pulses for the TPFS inverter. To achieve this, the FLC receives two essential inputs. The first input is the current error, which represents the deviation between the reference current (Iref) and the actual d-axis current (Id). This current error is a critical factor in determining the required voltage adjustment. The second input is the change in error (Δe), which is created by the memory block and provides valuable information about the rate of change of the current error. By processing these two inputs, the FLC produces the optimal voltage reference value. The inverter's actual currents are processed through Clarke's and Park's transformations to compute the Id and Iq currents. The reference current (I$_{ref}$) is derived from the DC-Link voltage and then compared with the actual currents to calculate the error. This error is subsequently fed into the FLC block, as illustrated in Figure 6.
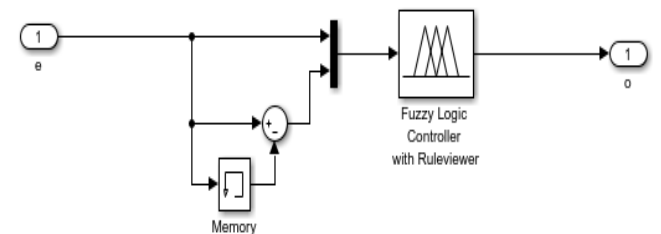

Figure 6 Flow diagram of implemented Fuzzy Logic Controller

The simplified FLC's fuzzy rule base maps input variables to outputs using fuzzy IF-THEN-AND logic rules with five linguistic expressions, as detailed in Table III. These linguistic variables are expressed by "Negative Large (NL)", "Negative Small (NM)", Zero (Z)"," Positive Small (PS)", and "Positive Large (PL)", for all variables. The Membership Functions (MFs) of two inputs are Id, I$_q$ error (e), de (change

in error), and Ud, Uq (voltage reference values) after selecting the scaling parameters, the membership functions (MFs) are determined, playing a crucial role in the FLC. Figure 7 illustrates the MFs used for both input and output fuzzy sets in generating reference voltages. Triangular MFs are chosen for all fuzzy sets due to their simple mathematical representation, which facilitates easier implementation of the fuzzy logic inference engine while minimizing computational complexity for real-time applications [25]-[26]. Figure 8 shows the surface viewer of FLC.

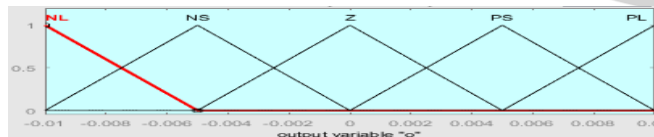**Table III   Rule Base for Five Membership Function**

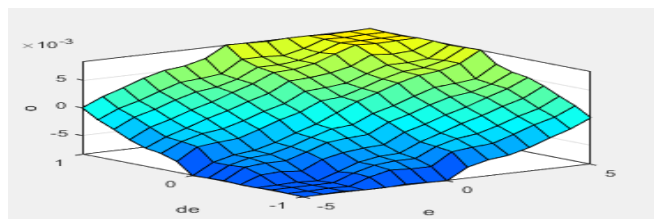| Change in Error(de)	Error (e)				
	NL	Ns	Z	PS	PL
NL	NL	NL	NL	NS	Z
NS	NL	NL	NS	Z	PS
Z	NL	NS	Z	PS	PL
PS	NS	Z	PS	PL	PL
PL	Z	PS	PL	PL	PL
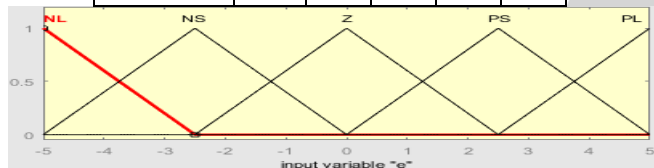
(a)
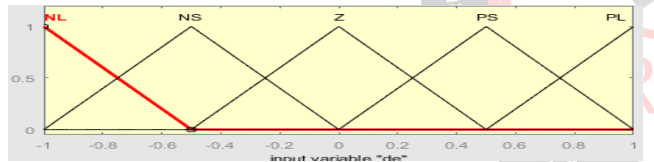
(b)

(c)

Figure 7 Membership functions for, (a) current error (e) , (b) change of current error de (c) voltage reference Ud Uq implemented in Matlab Simulink

**Figure 8 Surface Viewer**

## IV. SIMULATION AND RESULTS

In this section, Compares SRF-FLC with the conventional classic control method, SRF-PI. For this purpose, the SRF-PI Controller has been considered and simulated in MATLAB/Simulink. The PV model is connected to the TPFS inverter through the DC-Link and the output is connected to the three-phase utility grid via the Boost Converter.

However, the conventional PI controller introduces a higher ripple, resulting in harmonics in the inverter currents. Nevertheless, the inverter's voltage harmonics are relatively lower compared to the currents. Simulation response output voltage and current of a TPFS inverter using both the controller displayed in Figures 9 (a) and (b). The traditional SRF-based PI controller is shown in Figure 9(a) and the proposed SRF-based FL Controller is shown in Figure 9 (b). The output voltage of the SRF-FLC controller displays a sinusoidal waveform, showing a notable enhancement comparison to the SRF-PI controller. While the SRF-PI controller's output voltage contains harmonics and ripples, the SRF-FLC controller's output voltage remains smooth and sinusoidal, ensuring a higher quality of power delivery.
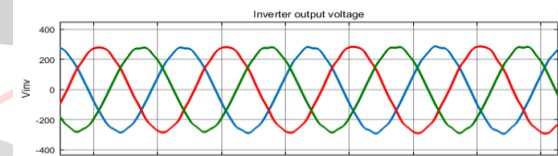

(a)
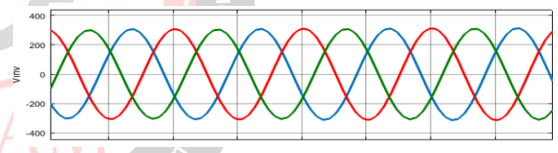
(b)

Figure 9: Simulation response of voltage and current of TPFS grid-connected PV inverter using (a) Traditional SRF-PI controller (b) Proposed SRF-FLC

The inverter voltages of both six-switch and four-switch are analyzed using the FFT analysis tool to determine the THD of the signal and are presented in Figure 10. The Total Harmonic Distortion (THD) for the TPSS inverter using the SRF-PI controller is noted to be 2.81%. THD for the proposed SRF-FL controller is 0.42% as recorded in Fig. 11. The analysis of voltages is carried out at the same time with the same rating of the system and PVA. It compensates with a significant power output to the grid, making it a suitable option for energy transfer. Therefore, the TPFS inverter performs better than the TPSS inverter, as it is more efficient. The performance of the TPFS inverter topology can be improved by the SRF-Fuzzy Logic controller. THD and injected power is delivered to the grid is improved by using SRF-FLC as discussed above.
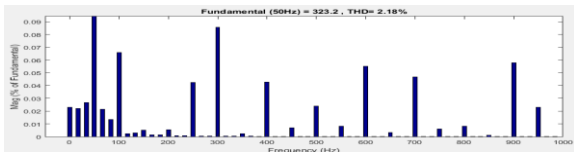
Figure 10: THD using SRF-PI controller for TPSS inverter
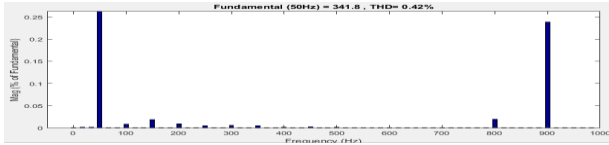
Figure 11: THD using SRF-FL Controller for TPFS inverter

V. Conclusion

This paper presents an SRF-FLC with PVA grid interconnection using different inverter topologies. The paper provides the design and modeling of the TPFS inverter, along with a mathematical model of the switching states. To synchronize the inverter, an SRF controller is used to generate reference signals for the four-switch SVPWM. The paper also carries out a comparative analysis between the SRF-PI and SRF-FLC of a four-switch inverter for the same system and PVA rating. The harmonic distortion of the SRF-PI controller for the TPSS inverter is 2.18% which is low as compared to the TPFS inverter which is calculated to be 3.54%, while the SRF-FLC for the TPFS inverter has a comparatively low harmonic distortion of 0.42% compared to SRF-PI Con trollers for both TPSS and TPFS inverters. Therefore, the Three-Phase Four-Switch inverter with SRF-FLC outperforms the SRF-PI controller, as it is more efficient and has fewer harmonics. The performance of the proposed topology can be further improved by updating the controllers.

References

[1] S. Takijawa, M. Tabata, T. Tanigawa, S. Igarashi, and K. Kuroki, "High-efficiency drive techniques for the brushless DC motor using a four switch, three-phase inverter," in Proc. Int. Power Electronic Conf. (IPEC), Tokyo, Japan, 2000, pp. 1692–1697.

[2] J. S. Larsen, K. Jespersen, M. R. Pedersen, F. Blaabjerg, and J. K. Pedersen, "Control of a complete digital based component-minimized single-phase to three-phase AC/DC/AC converter," in Proc. IEEE Industrial Electronics Society (IECON) Conf., Aachen, Germany, 1998, pp. 618–625.

[3] H. W. Van der Broeck and J. D. Van Wyk, "A comparative investigation of a three-phase induction machine drive with a component minimized voltage-fed inverter under different control options," IEEE Trans. Ind.Appl., vol. IA20, no. 2, pp. 309–320, Mar. 1984.

[4] R. Wang, J. Zhao, and Y. Liu, "DC-link capacitor voltage fluctuation analysis of four-switch three-phase inverter," in Proc. Conf. Rec. IEEE Ind. Electron. Soc., 2011, pp. 1276–1281.

[5] H. Zhang, "Imbalance Compensation for SVPWM-Controlled Four-switch Three-phase Inverters," 2023 IEEE Green Technologies Conference (Greentech), Denver, CO, USA, 2023, pp. 95-100, doi: 10.1109/GreenTech56823.2023.10173831.

[6] F. Blaabjerg, Dorin O. Neacsu, John K. Pedersen "Adaptive SVM to Compensate DC-Link Voltage Ripple for Four-Switch Three- Phase VSI" IEEE Trans. on Power Electronics, Vol. 14, No. 4, Jul. 1999, pp 743-752.

[7] H. Zhang, "A Simplified Space Vector PWM Algorithm for Four-Switch Three-phase Inverters," 2021 IEEE 12th International Symposium on Power Electronics for Distributed Generation Systems (PEDG), Chicago, IL, USA,   2021,pp.1-6,doi: 10.1109/PEDG51384.2021.9494166.

[8] M. Masiala, B. Vafakhah, J. Salmon, and A. M. Knight, "Fuzzy self-tuning speed control of an indirect field-oriented control induction motor drive," IEEE Trans. Ind. Appl., vol. 44, no. 6, pp. 1732–1739, Nov./Dec. 2008.

[9] A. Saghafinia, H. Wooi Ping, M. Nasir Uddin, and K. Salloum Gaeid, "Adaptive fuzzy sliding-mode control into chattering-free IM drive," IEEE Trans. Ind. Appl., vol. 51, no. 1, pp. 692–701, Jan./Feb. 2015.

[10] Eshkevari, Alireza Lahooti; Mosallanejad, Ali, and Sepasian,   Mohammad Sadegh (2020) "A new configuration for four-switch three-phase inverters based on a switched-capacitor step-up cell for electric vehicles application," Turkish Journal of Electrical Engineering and Computer Sciences: Vol. 28: No. 6, Article 21. https://doi.org/10.3906/elk-2005-141.

[11] Sowilam, Gamal. (2015). Six-Space Vector Pulse Width Modulation of Four-Switch Voltage Source Inverter Feeding Three Phase Induction Motor. 10.13140/RG.2.1.3864.7522.

[12] P. Q. Dzung, Le Minh Phuong, P. Q. Vinh, N. M. Hoang and T. C. Binh, "New Space Vector Control Approach for Four Switch Three Phase Inverter (FSTPI)," 2007 7th International Conference on Power Electronics and Drive Systems, Bangkok, Thailand, 2007, pp. 1002-1008, doi: 10.1109/PEDS.2007.4487826.

[13] Phan Quoc Dzung, Le Minh Phuong, Hong Hee Lee, Bui Ngoc Thang and Le Dinh Khoa, "A new FPGA implementation of four- switch three- phase inverter," 2009 International Conference on Power Electronics and Drive Systems (PEDS), Taipei, Taiwan, 2009, pp. 882-887, doi: 10.1109/PEDS.2009.5385825.

[14] Kivanc, O.C. and Ozturk, S.B. (2017), Sector determination for SVPWM based four-switch three-

phase VSI. Electron. Lett., 53: 343-345. https://doi.org/10.1049/el.2016.3711

[15] A. Durgadevi, S. Arulselvi and S. P. Natarajan, "Photovoltaic modeling and its characteristics," *2011 International Conference on Emerging Trends in Electrical and Computer Technology*, Nagercoil, India, 2011, pp. 469-475, doi: 10.1109/ICETECT.2011.5760162.

[16] D. Jiandong, X. Ma and S. Tuo, "A Variable Step Size P&O MPPT Algorithm for Three-Phase Grid-Connected PV Systems," *2018 China International Conference on Electricity Distribution (CICED)*, Tianjin, China, 2018, pp. 1997-2001, doi: 10.1109/CICED.2018.8592040.

[17] K. S. Fuad, E. Hossain, and M. R. U. Chowdhury, "Grid-voltage synchronization algorithm for grid-tied renewable energy sources during adverse grid fault condition," 2016 International Conference on Innovations in Science, Engineering, and Technology (ICISET), Dhaka, Bangladesh, 2016, pp. 1-5, doi: 10.1109/ICISET.2016.7856524.

[18] S.Chatterjee and S. Chatterjee, "Simulation of synchronous reference frame PLL based grid-connected inverter for photovoltaic application," *2015 1st Conference on Power, Dielectric and Energy Management at NERIST (ICPDEN)*, Itanagar, India, 2015, pp. 1-6, doi: 10.1109/ICPDEN.2015.7084493.

[19] X. Quan and A. Q. Huang, "PI-Based Synchronous Reference Frame Frequency-Locked Loop," in *IEEE Transactions on Industrial Electronics*, vol. 68, no. 5, pp. 4547-4553, May 2021, doi: 10.1109/TIE.2020.2985002.

[20] Masri, Syafrudin & Aphieez, H & Rosa Susila, Jaya Kuncara. (2021). Modeling and Performance Analysis of Synchronous Reference Frame Phase-Locked Loop for Three-phase Grid-connected PV Generation System. Journal of Physics: Conference Series. 1764. 012169. 10.1088/1742-6596/1764/1/012169.

[21] A. H. Chander and L. Kumar, "Design of a Synchronous Reference Frame Controller for Single Phase Standalone Photovoltaic Inverter," *2017 14th IEEE India Council International Conference (INDICON)*, Roorkee, India, 2017, pp. 1-6, doi: 10.1109/INDICON.2017.8487990.

[22] Y. P. Bhatt and M. C. Shah, "Design, analysis and simulation of synchronous reference frame based Phase Lock Loop for grid connected inverter," *2016 IEEE 1st International Conference on Power Electronics, Intelligent Control and Energy Systems (ICPEICES)*, Delhi, India, 2016, pp. 1-5, doi: 10.1109/ICPEICES.2016.7853618.

[23] Costa, I.D.L.; Brandao, D.I.; Matakas Junior, L.; Simões, M.G.; Morais, L.M.F. Analysis of Stationary- and Synchronous-Reference Frames for Three-Phase Three-Wire Grid-Connected Converter AC Current Regulators. *Energies* **2021**, *14*, 8348. https://doi.org/10.3390/en14248348.

[24] S. Golestan, J. M. Guerrero and J. C. Vasquez, "A PLL-Based Controller for Three-Phase Grid-Connected Power Converters," in *IEEE Transactions on Power Electronics*, vol. 33, no. 2, pp. 911-916, Feb. 2018, doi: 10.1109/TPEL.2017.2719285.

[25] Jae-Sung Yu, Sang-Hoon Kim, Byoung-Kuk Lee, Chung-Yuen Won, and Jin Hur "Fuzzy-Logic-Based Vector Control Scheme for PermanentMagnet Synchronous Motors in Elevator Drive Applications" IEEE Transactions on Industrial Electronics, Vol. 54, No. 4, pp. 2190-2200, August 2007

[26] M. N. Uddin, and and Ronald S. Rebeiro, "Online Efficiency Optimization of a Fuzzy-Logic-Controller-Based IPMSM Drive," IEEE Transactions on Industry Applications, 2011, 47, (2), pp. 1043-1050.